apparently because of geometric constraints.

The structural difference between the palladium complex on the one hand and the nickel and platinum complexes on the other clearly illustrate the fact that, of the three zerovalent metals of the triad, palladium has the lowest affinity for olefins. Spectroscopic and chemical evidence suggests that even the one coordinated vinyl group of $Pd(SP)_2$ is more weakly bound than the vinyl groups of $Ni(SP)_2$ and $Pt(SP)_2$. Thus, the ^1H and ^{13}C nuclei of the coordinated vinyl groups of **4** are less shielded than those of $Ni(SP)_2$ and $Pt(SP)_2$, even at −80 °C, where the exchange between free and coordinated vinyl groups has been slowed, and the C=C distance and bend-back angle of the coordinated vinyl group in **4** is somewhat less than those in $Ni(SP)_2$ and $Pt(SP)_2$. In solution, the three-coordinate, 16e species present in the solid state is in equilibrium with an isomer which contains essentially two-coordinate, 14e palladium(0), although the "free" vinyl groups may interact weakly with the metal atom. Finally, the coordinated vinyl group of **4** is easily displaced by more SP to give $Pd(SP)_3$ (**5**), whereas the nickel(0) and platinum(0) analogues of **5** could not be made.

It has been shown[50] that the binding of ligands to the zerovalent d^{10} elements can be correlated with the difference between the electron affinity (EA) and the $d^{10} \rightarrow d^9$ ionization potential of the elements. The electron affinity should parallel the tendency to form a strong σ-bond, whereas the ionization potential should correlate with the π-back-bonding ability. On this basis, the σ-bond strength is in the order Pt > Pd ≃ Ni and the π-bond strength is in the order Ni > Pt ≃ Pd. The order of (EA − IP) is Ni > Pt > Pd, palladium(0) apparently being relatively weak at both σ- and π-bonding. The M–P distance in **4** [2.304 Å (av)] is significantly larger than that in $Pt(SP)_2$ [2.284 Å (av)], and a similar trend is evident from comparison of $Pd(P\text{-}t\text{-}Bu_2Ph)_2$ [Pd–P = 2.285 (2) Å] with $Pt(P\text{-}t\text{-}Bu_2Ph)_2$ [Pt–P = 2.252(1) Å]. Otsuka et al.[25,46] have estimated the covalent radii of Pd(0) and Pt(0) to be 1.35 and 1.38 Å, respectively, so the trend in M–P distances probably reflects the greater σ-bond strength of Pt(0)–P relative to Pd(0)–P.

As discussed in the previous paper,[9] the affinity of the divalent metal ions of the nickel triad for olefins is in the order Pt > Pd > Ni, so the fact that compound **6** formed by protonation of **4** is much more stable than the corresponding nickel compound is not surprising.

Finally, we note that the electron deficiency of $Pd(SP)_2$ causes it to be much more reactive than either $Ni(SP)_2$ or $Pt(SP)_2$ in oxidative addition reactions with organic halides; these reactions are described elsewhere.[51]

Acknowledgment. We thank Lee Welling for technical assistance and K. D. Griffiths for computational assistance.

Registry No. **3**, 113509-37-8; **4**, 113509-38-9; **5**, 113509-39-0; **6**, 113509-41-4; $Pd(\eta^3\text{-}C_3H_5)(\eta^5\text{-}C_5H_5)$, 1271-03-0.

Supplementary Material Available: A table of comparative bond lengths and bond angles for $M(o\text{-}CH_2{=}CHC_6H_4PPh_2)_2$ (M = Ni, Pd, Pt) and tables of anisotropic thermal parameters and hydrogen atom parameters for $Pd(o\text{-}CH_2{=}CHC_6H_4PPh_2)_2$ (**4**) (7 pages); a listing of structure factor amplitudes for **4** (29 pages). Ordering information is given on any current masthead page.

(50) De Kock, R. L. *Inorg. Chim. Acta* **1976**, *19*, L27.

(51) Bennett, M. A.; Kapoor, P. N. *J. Organomet. Chem.*, in press.

Group VI Open-Mode Dimers Based on a Binucleating Hexaphosphine Ligand System. Synthesis and Conformational Studies of *fac*,*fac*-$M_2(CO)_6$(eHTP) (M = Cr, Mo, W; eHTP = $(Et_2PCH_2CH_2)_2PCH_2P(CH_2CH_2PEt_2)_2$)

Suzanne E. Saum,[1a] Fredric R. Askham,[1a] Frank R. Fronczek,[1b] and George G. Stanley*[1b]

Departments of Chemistry, Louisiana State University, Baton Rouge, Louisiana 70803-1804, and Washington University, St. Louis, Missouri 63130

Received December 15, 1987

The reaction of 2 equiv of $M(CO)_6$ (M = Cr, Mo, W) with the hexatertiary phosphine $(Et_2PCH_2CH_2)_2PCH_2P(CH_2CH_2PEt_2)_2$, eHTP, in refluxing xylene yields the binuclear complexes $M_2(CO)_6$(eHTP) (M = Cr, Mo, W). These complexes have been characterized by IR and ^1H and ^{31}P NMR spectroscopy, elemental analysis, and X-ray crystallography. All three compounds are isomorphous and crystallize in the orthorhombic space group *Pcca* (Z = 4) with the following crystal data. Cr: a = 29.890 (4) Å, b = 8.102 (2) Å, c = 16.346 (2) Å, V = 3958 (2) Å^3. Mo: a = 30.353 (3) Å, b = 8.153 (3) Å, c = 16.497 (2) Å, V = 4083 (2) Å^3. W: a = 30.324 (3) Å, b = 8.137 (1) Å, c = 16.471 (6) Å, V = 4064 (2) Å^3. The final discrepancy indices (R values) for these three structures are 0.038, 0.037, and 0.036, with quality of fit indicators of 1.15, 1.33, and 1.05 for the Cr, Mo, and W structures, respectively. The three dimer systems lie on a twofold rotation axis that passes through the central eHTP methylene bridge and have symmetric open-mode structures with M–M separations of 6.2872 (8) (Cr), 6.4687 (5) (Mo), and 6.4687 (5) Å (W). The local geometry about each metal center is a facial set of three carbonyl and three phosphine ligands with the expected angular deviations away from pure octahedral geometry caused by the tridentate phosphine donor set. Spectroscopic evidence and the results from van der Waals energy calculations are presented to show that the rotational conformation of these dimers about the eHTP methylene bridge in solution is different from that seen in the solid-state crystal structures.

Fragmentation remains a persistent problem in multimetallic complexes and continues to be a major stumbling block to the development of these species as homogeneous catalysts. We have approached the fragmentation and

0276-7333/88/2307-1409$01.50/0 © 1988 American Chemical Society

synthetic problems traditionally associated with dimer and cluster systems by designing a new type of polyphosphine ligand capable of both bridging and chelating two transition-metal centers. The ligand system $(Et_2PCH_2CH_2)_2PCH_2P(CH_2CH_2PEt_2)_2$, abbreviated eHTP

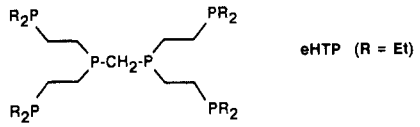

eHTP (R = Et)

(for *ethyl*-substituted *hexatertiary phosphine*), has a central bis(phosphino)methane linkage which prefers bridging two metal centers, while the (dialkylphosphino)ethyl arms favor chelation to the two metal atoms. This ligand can be best viewed as a combination of two tridentate bischelating phosphine units. Importantly, eHTP can be prepared in large quantities via a high yield synthetic route that is amenable to modifications to produce a number of variations in the basic structure of the polyphosphine ligand to fine tune both steric and electronic effects.[2]

eHTP was designed to form closed-mode binuclear complexes of the general type **1a** shown below, and we have spectroscopically characterized this closed-mode geometry for the Co(0) dimer $Co_2(CO)_2$(eHTP).[3] It has been found, however, that open-mode complexes of types **1b**, **1c**, and **1d** can also be produced. We initially reported the syn-

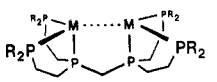

1a

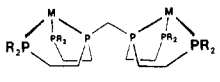

1b

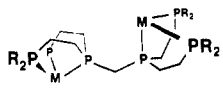

1c

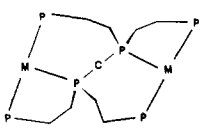

1d

thesis and characterization of the open-mode cobalt dimers Co_2Cl_{4-x}(eHTP)$^{x+}$ (x = 0 or 2) and $Co_2(CO)_4$(eHTP)$^{2+}$ and the crystallographic characterization of the latter complex which has the eHTP conformation **1b**.[2] This inverted, W-shaped geometry for a bis(phosphino)methane based linkage was, until very recently, unprecedented with respect to both its orientation and the rather large P–CH_2–P angle (127.7 (3)°) present. Singleton and co-workers have reported the first example of a transition-metal dimer system with a bis(diphenylphosphino)methane (dppm) ligand that has this inverted P–CH_2–P orientation, namely, $[\{(\eta^5\text{-}C_5H_5)Ru(1,10\text{-phen})\}_2(\mu\text{-dppm})]^{2+}$, which has the remarkable P–CH_2–P angle of 133.1 (3)°.[4] In order to better understand the conformational preferences of eHTP, our initial work has concentrated on probing the structure and dynamics of a variety of transition-metal eHTP dimer complexes where the metal centers will be adopting different coordination numbers and geometries.

The four-coordinate nickel(II) complex Ni_2Cl_2(eHTP)$^{2+}$, for example, shows considerable rotational flexibility about the P–CH_2–P bridge with the result that we have crystallographically characterized both open-mode conformations **1c** and one rotated about 50° away.[5] In marked contrast to the nickel system, the isoelectronic palladium(II) and platinum(II) complexes M_2Cl_2(eHTP)$^{2+}$ have partially closed-mode configurations with M–M separations of 4.4217 (8) and 4.6707 (9) Å for Pd and Pt, respectively.[6,7] The Pt dimer has a remarkably expanded central P–CH_2–P angle of 129.7 (9)° which puts it in rather select company for large angles observed about a methylene bridge.[4,8] We do not yet fully understand why the Pd/Pt dimers adopt this conformation or unusually large methylene bridge angles when they could rotate into one of the ligand configurations seen for the nickel system which have smaller P–CH_2–P bridge angles around 122°.

The reaction of 2 equiv of $CrCl_3$·3THF with eHTP, on the other hand, gives the paramagnetic Cr(III) dimer *mer,mer*-Cr_2Cl_6(eHTP) which has the unusual open-mode conformation **1d**.[9] This rather unexpected eHTP geometry results from the electronic preference of a Cr(III) center to have a meridional arrangement of three phosphine and halide ligands.[10] The long P–Cr bond distances in this complex, however, would introduce considerable steric strain for a symmetrically coordinated eHTP ligand with two transoidally fused five-member ring systems, like that seen for our M_2Cl_2(eHTP)$^{2+}$ complexes or the very similar mononuclear Cr(III) complex $CrCl_3$(tetraphos) (tetraphos = $P(CH_2CH_2PPh_2)_3$),[10] while the adoption of conformation **1d** avoids many of these unfavorable steric factors.

It has become clear from our work so far that eHTP is a powerful binucleating ligand for transition-metal centers and exhibits a considerable amount of flexibility, both in its coordination geometries and in the bending of the central methylene bridge. Although we have gained a relatively good idea about the type of dimer complexes we can expect with eHTP, more structural work is clearly needed to get us to the point of being able to more confidently predict eHTP conformations and understand the dynamics of rotations about the central methylene bridge. We would, therefore, like to report the preparation of an isomorphous series of dimer systems $M_2(CO)_6$(eHTP) (M = Cr, Mo, W), their structural characterization, and the results of conformational studies on the rotational preferences of these systems.

Experimental Section

All manipulations were carried out under inert atmosphere (N_2 or Ar) by using standard Schlenk or glovebox techniques unless stated otherwise. Solvents were distilled under inert atmosphere from the following drying agents: diethyl ether, hexane, and THF (sodium/benzophenone); toluene (sodium); CH_2Cl_2 and acetonitrile (CaH_2); methanol and ethanol (magnesium). $Cr(CO)_6$, $Mo(CO)_6$, and $W(CO)_6$ (Strem Chemicals), sodium and potassium (Alfa division of Morton Thiokol), and xylene and cycloheptatriene (Aldrich) were used as received without further purification. eHTP was prepared according to published procedures.[2] ^1H and ^{31}P NMR spectra were run on a Varian XL-300 spectrometer, IR spectra were run on a Perkin-Elmer 283B spectrometer, NMR simulations were done on a Bruker Aspect 2000 stand alone data

(1) (a) Washington University. (b) LSU.
(2) Askham, F. R.; Stanley, G. G.; Marques, E. C. *J. Am. Chem. Soc.* **1985**, *107*, 7423.
(3) D'Avignon, A.; Askham, F. R.; Stanley, G. G., manuscript in preparation.
(4) Albers, M. O.; Liles, D. C.; Robinson, D. J.; Singleton, E. *Organometallics* **1987**, *6*, 2179.
(5) Laneman, S. A.; Stanley, G. G. *Inorg. Chem.* **1987**, *26*, 1177.
(6) Saum, S. E.; Stanley, G. G. *Polyhedron* **1987**, *6*, 1803.
(7) Saum, S. E.; Laneman, S. A.; Stanley, G. G., manuscript in preparation.
(8) Johnson, C. A.; Guenzi, M.; Nachbar, R. B., Jr.; Blount, J. F.; Wennerstrom, O.; Mislow, K. *J. Am. Chem. Soc.* **1982**, *104*, 5163.
(9) Askham, F. R.; Maverick, A. W.; Stanley, G. G. *Inorg. Chem.* **1987**, *26*, 3963.
(10) Gray, L. R.; Hale, A. L.; Levason, W.; McCullough, F. P.; Webster, M. *J. Chem. Soc., Dalton Trans.* **1984**, 47.

station using the simulation program PANIC, and elemental analyses were performed by Galbraith Laboratories, Inc., Knoxville, TN.

$Cr_2(CO)_6$(eHTP) (2) (Method A). eHTP (0.200 g, 0.368 mmol) was diluted with 75 mL of hexane and added quickly to $Cr(CO)_3$(cycloheptatriene) (0.170 g, 0.746 mmol).[11] The purple reaction mixture was refluxed, and a yellow solid began to precipitate after 10 min and continued until the solution color had become light yellow. The solid was collected by filtration and washed with hexane to give 0.241 g of crude material. ^{31}P NMR shows that the desired compound makes up approximately 50% of this yellow material giving an overall crude yield of 40%. This mixture was washed with cold acetone until the yellow color was removed. The remaining white solid was dissolved in CH_2Cl_2, filtered to remove sediment, and crystallized by slow evaporation of the solvent (0.032 g, 10% recrystallized yield). **2** is a diamagnetic, air-stable product.

Method B. eHTP (0.300 g, 0.55 mmol) and $Cr(CO)_6$ (0.291 g, 1.10 mmol) were added to 50 mL of xylene, and the solution was refluxed for 2 days, over which a white precipitate formed. The solution was then allowed to cool and the volume vacuum evaporated to approximately 20 mL. The white solid was collected by filtration to give 0.577 g of $Cr_2(CO)_6$(eHTP) (64% yield). Recrystallization from CH_2Cl_2/toluene gives X-ray quality single crystals. The only common solvent that **2** was soluble in was CH_2Cl_2.

Anal. Calcd for $C_{31}H_{58}Cr_2O_6P_6$: C, 45.59; H, 7.16; O, 11.76; P, 22.76. Found: C, 45.31; H, 7.14; O, 11.59; P, 21.89. IR (KBr): 2970, 2940, 2910, 2880 (m, CH), 1920, 1820, 1800 (vs. CO), 1460, 1420 (m, CH), 1380 (w, CH), 1040, 1030 (m, PEt), 895 (w), 858 (w), 810 (m, br), 790 (m), 768 (m), 750 (m), 733 (w), 712 (w), 703 (w), 680 (m), 660 (w), 640 (m), 633 (m), 615 (w), 550 (m) cm^{-1}. $^{31}P\{^1H\}$ NMR (CD_2Cl_2, ppm, H_3PO_4 reference): 72.7 (m, 4 P), 107.0 (m, 2 P). ^{31}P coupling constants from $A_2XX'A'_2$ simulation (Hz): 23.5 (P_{int}–P_{int}), 16.8 (P_{int}–P_{ext}). ^1H NMR (CD_2Cl_2, ppm, TMS reference): 1.08–1.20 (m, P–CH_2CH_3), 1.50–1.96 (m, P–CH_2CH_3 and chelate ring hydrogen atoms), 2.10–2.24 (m, br, chelate ring hydrogen atoms), 2.58 (t, P–CH_2–P, J_{P-H} = 8 Hz).

$Mo_2(CO)_6$(eHTP) (3). This compound was prepared by the same procedure used for **2** (method B) to give white $Mo_2(CO)_6$(eHTP) in a recrystallized yield of 41%. As with **2**, **3** is only soluble in CH_2Cl_2.

Anal. Calcd for $C_{31}H_{58}Mo_2O_6P_6$: C, 41.16; H, 6.46; P, 20.54; O, 10.61. Found: C, 41.22; H, 6.76; P, 20.19; O, 10.98. IR (KBr): 2970, 2940, 2920, 2880 (m, CH), 1924, 1833, 1810 (vs, CO), 1460, 1430, 1420, 1380 (m-w, CH), 1250 (w, br), 1040, 1030 (m, P–Et), 892 (w), 852 (w), 822 (w), 807 (w, br), 790 (w), 765 (m), 748 (ms), 728 (m), 710 (m), 700 (m), 660 (w), 610 (m), 600 (w), 585 (w), 574 (w), 510 (m) cm^{-1}. $^{31}P\{^1H\}$ NMR (CD_2Cl_2, ppm, H_3PO_4 reference): 75.2 (m, 2 P), 52.6 (d, 4 P, J_{P-P} = 5 Hz). ^1H NMR (CD_2Cl_2, ppm, TMS reference): 1.1–1.22 (m, P–CH_2CH_3), 1.44–2.0 (m, P–CH_2CH_3 and chelate ring hydrogen atoms), 2.16–2.26 (m, br, chelate ring hydrogen atoms), 2.51 (t, P–CH_2–P, J_{P-H} = 8 Hz).

$W_2(CO)_6$(eHTP) (4). This compound was prepared by the same procedure used for **2** (method B) to give white $W_2(CO)_6$(eHTP) in a recrystallized yield of 39%. As with **2** and **3**, **4** is only soluble in CH_2Cl_2.

Anal. Calcd for $C_{31}H_{58}W_2O_6P_6$ (**4**): C, 34.46; H, 5.41; P, 16.77; O, 8.88. Found: C, 34.32; H, 5.40; P, 17.20; O, 9.57. IR (KBr): 2970, 2940, 2920, 2880 (m, CH), 1920, 1827, 1805 (vs, CO), 1460, 1430, 1420, 1382 (m-w, CH), 1255 (w, br), 1090, 1040 (m, P–Et), 980 (w), 895 (w), 852 (w), 818 (m), 765 (m), 749 (m), 730 (m), 712 (m), 702 (m), 670 (w), 620 (m, br), 590 (w), 575 (w), 512 (m) cm^{-1}. $^{31}P\{^1H\}$ NMR (CD_2Cl_2, ppm, H_3PO_4 reference): 62.6 (s, 2 P, J_{W-P} = 203 Hz), 36.1 (s, 4 P, J_{W-P} = 209 Hz). ^1H NMR (CD_2Cl_2, ppm, TMS reference): 1.08–1.20 (m, P–CH_2CH_3), 1.5–2.0 (m, P–CH_2CH_3 and chelate ring hydrogen atoms), 2.1–2.27 (m, br, chelate ring hydrogen atoms), 2.55 (t, P–CH_2–P, J_{P-H} = 9 Hz).

SYBYL van der Waals Energy Calculations. The crystallographic coordinates of **3** were input into the SYBYL program set (version 3.4) and the terminal ethyl groups replaced by methyl groups. Idealized hydrogen atom positions were calculated from within SYBYL and added to the molecule. The two central phosphorus methylene bonds were selected for rotation, and the initial van der Waals screening factors were set at 50% of the default values. van der Waals energies (no electrostatic effects were included) were calculated for each 5° rotational increment and a two-dimensional contour map of the results plotted off.

The calculation on King's $M_2(CO)_6\{P_2(\text{-}Pf_4)\}$ complex used the model system described above with a central ethylene bridge instead of a methylene group. The bond distances and angles about the central ethylene bridge were adjusted manually to give reasonable bond distances and angles. The three central bonds (P1–C1, C1–C1′, and P1′–C1′) on the central ethylene group were selected for rotation with an angular increment of 30°.

Table I. Crystallographic Data for $M_2(CO)_6$(eHTP) (M = Cr, Mo, and W)

	Cr	Mo	W
Crystal Parameters			
formula	$Cr_2P_6O_6C_{31}H_{58}$	$Mo_2P_6O_6C_{31}H_{58}$	$W_2P_6O_6C_{31}H_{58}$
fw	816.64	904.53	1080.35
crystal system	orthorhombic	orthorhombic	orthorhombic
space group	*Pcca*	*Pcca*	*Pcca*
a, Å	29.890 (4)	30.353 (3)	30.324 (3)
b, Å	8.102 (2)	8.153 (3)	8.137 (1)
c, Å	16.346 (2)	16.497 (2)	16.471 (6)
V, Å^3	3958 (2)	4083 (2)	4064 (2)
Z	4	4	4
d_{calcd}, g/mL	1.37	1.47	1.76
μ(Mo Kα), cm^{-1}	8.11	8.67	60.48
temp, °C	23	23	23
cryst size, mm	0.40 × 0.28 × 0.20	0.24 × 0.22 × 0.14	0.20 × 0.18 × 0.11
cryst color	v. pale green	colorless	colorless
Data Collection and Structure Refinement			
diffractometer	CAD4	CAD4	CAD4
radiation	Mo Kα	Mo Kα	Mo Kα
monochromator	graph. cryst	graph. cryst	graph. cryst
attenuator	17.5	17.5	17.5
scan method	$\theta/2\theta$	$\theta/2\theta$	$\theta/2\theta$
variable scan speed, deg/min	0.5–4	0.5–4	1–4
data limits, deg	$3 < 2\theta < 55$	$3 < 2\theta < 60$	$3 < 2\theta < 60$
octants collcd	*h*,*k*,*l*	*h*,*k*,*l*	*h*,*k*,*l*
no. of reflcns collcd	5376	6645	6621
no. of unique data $F_o^2 > 3\sigma(F_o^2)$	2906	3292	3401
weighting scheme	non-Poisson	non-Poisson	non-Poisson
fudge factor, *P*	0.06	0.04	0.07
no. of params refined	319	320	204
data/param ratio	9.1	10.3	16.7
R^a	0.038	0.037	0.036
$R_w{}^b$	0.048	0.041	0.051
GOF^c	1.15	1.33	1.05
largest final Fourier peak, e/Å^3	0.34	0.60	1.19
largest final shift/esd	0.03	0.08	0.00
abs cor	yes	yes	yes
min transmissn coeff	0.8298	0.8982	0.5249

$^a R = \sum||F_o| - |F_c||/\sum|F_o|$. $^b R_w = [\sum w(|F_o| - |F_c|)^2/\sum w|F_o|^2]^{1/2}$; $w = 1/\sigma^2(|F_o|)$. ^{c} Goodness of fit = $[\sum w(|F_o| - |F_c|)^2/(N_o - N_{param})]^{1/2}$.

X-ray Crystallographic Procedure. Data were collected on an Enraf-Nonius CAD4 diffractometer at room temperature using Mo Kα radiation and a graphite crystal monochromator by $\theta/2\theta$ scan technique using variable speed scanning rates. The choice of $\theta/2\theta$ scans and the presence of 30-Å crystallographic *a* axis in the structures did not give any problems with overlapping reflections since the peaks were quite narrow. Furthermore, the worst overlap problem would have been with the collection of the *h*00 peaks, but fortunately, in the *Pcca* space group the *h*00 (*h* = odd) reflections are absent so there were not any difficulties in the collection of the *h*00 (*h* = even) peaks. Crystal data and experimental details are listed in Table I. Data reduction included corrections for background, Lorentz, and polarization effects, as well as an empirical absorption correction based on ϕ scans of reflections near χ = 90°.

The chromium structure was solved by location of the Cr atom from a Patterson map followed by full-matrix least-squares re-

(11) King, R. B. *J. Organomet. Chem.* **1967**, *8*, 139.

Table II. Positional Parameters for $Cr_2(CO)_6(eHTP)$[a]

atom	x	y	z	B, Å²
Cr	0.14484 (1)	0.00506 (6)	−0.01410 (3)	2.152 (8)
P1	0.20323 (2)	0.1089 (1)	0.06694 (5)	2.07 (1)
P2	0.15795 (3)	0.2560 (1)	−0.08650 (5)	2.36 (1)
P3	0.09908 (3)	0.1283 (1)	0.08717 (5)	2.76 (2)
O1	0.06471 (9)	−0.1000 (4)	−0.1113 (2)	6.49 (8)
O2	0.1427 (1)	−0.3128 (3)	0.0784 (2)	5.55 (7)
O3	0.19600 (9)	−0.1862 (4)	−0.1391 (2)	4.72 (6)
C′	0.250	0.000	0.1178 (3)	2.49 (8)
C1	0.0951 (1)	−0.0535 (5)	−0.0742 (2)	3.80 (8)
C2	0.1431 (1)	−0.1873 (4)	0.0432 (2)	3.22 (7)
C3	0.1782 (1)	−0.1062 (4)	−0.0906 (2)	2.94 (6)
C11	0.2315 (1)	0.2814 (4)	0.0171 (2)	2.76 (6)
C12	0.1979 (1)	0.3866 (4)	−0.0292 (2)	2.96 (6)
C13	0.1794 (1)	0.2012 (5)	0.1610 (2)	3.12 (7)
C14	0.1327 (1)	0.2712 (5)	0.1492 (2)	3.68 (7)
C21	0.1158 (1)	0.4143 (4)	−0.1114 (2)	3.44 (7)
C22	0.0794 (1)	0.3543 (6)	−0.1698 (3)	5.3 (1)
C23	0.1856 (1)	0.2262 (4)	−0.1859 (2)	3.23 (7)
C24	0.1953 (2)	0.3776 (5)	−0.2374 (2)	4.62 (9)
C31	0.0760 (1)	−0.0096 (6)	0.1646 (2)	4.40 (8)
C32	0.0410 (1)	−0.1294 (6)	0.1345 (3)	5.6 (1)
C33	0.0494 (1)	0.2523 (6)	0.0585 (3)	5.2 (1)
C34	0.0272 (2)	0.3499 (7)	0.1259 (4)	7.7 (1)

[a] Anisotropically refined atoms are given in the form of the isotropic equivalent displacement parameter defined as $(^4/_3)[a^2B(1,1) + b^2B(2,2) + c^2B(3,3) + ab(\cos\gamma)B(1,2) + ac(\cos\beta)B(1,3 + bc(\cos\alpha)B(2,3)]$.

finement using data with $F_o^2 > 3\sigma(F_o^2)$, followed by identification of the other non-hydrogen atoms from difference Fourier maps. Non-hydrogen atoms were anisotropically refined, and all hydrogen atoms were subsequently located from difference Fourier maps with both positional and isotropic thermal parameters (except for H342 which was assigned a fixed isotropic thermal parameter of 10.0) were successfully refined to give the final discrepancy indices. Positional parameters for the non-hydrogen atoms are listed in Table II.

The molybdenum and tungsten structures proved to be isomorphous with the Cr system and were solved by using the fractional coordinates from the chromium structure as a starting point for refinement (for the tungsten structure, the coordinates from the molybdenum system were used). All non-hydrogen atoms were refined with anisotropic thermal parameters with all hydrogen atoms subsequently found from difference Fourier maps for the Mo structure, and both positional and isotropic thermal parameters were successfully refined. Only a few hydrogen atoms could be found in the tungsten structure, so they were all calculated into place and included in the final structure factor calculation. Positional parameters for the non-hydrogen atoms for the Mo and W structures are listed in Tables III and IV.

Tables of anisotropic thermal parameters, hydrogen positional parameters for the Cr and Mo structures, and observed and calculated structure factors for all three structures are included in supplementary information.

Results and Discussion

The reactions of two equivalents of $M(CO)_6$ (M = Cr, Mo, W) with eHTP produces the dimer species $Cr_2(CO)_6(eHTP)$ (**2**), $Mo_2(CO)_6(eHTP)$ (**3**), and $W_2(CO)_6(eHTP)$ (**4**). These complexes have infrared spectra which show two primary bands in the carbonyl region, consistent with a facial C_{3v} local symmetry, but since the doubly degenerate e band is split into two distinct peaks, it indicates that there is some definite lowering of the local symmetry (Figure 1). This could be a natural consequence of the somewhat asymmetric nature of each bischelating half of the eHTP ligand that lowers the local symmetry about the metal atoms below ideal C_{3v}. This, however, is probably *not* the case since other mononuclear $M(CO)_3(P_3)$ complexes based on $R_2PCH_2CH_2P(R)CH_2CH_2PR_2$ ligand systems with facial geometries are known and exhibit only two (a_1 and e modes) carbonyl bands.[12] The presence of

Table III. Positional Parameters for $Mo_2(CO)_6(eHTP)$

atom	x	y	z	B, Å²
Mo	0.14348 (1)	−0.01094 (3)	−0.01809 (2)	2.421 (5)
P1	0.20369 (3)	0.1039 (1)	0.06688 (5)	2.40 (2)
P2	0.15866 (3)	0.2554 (1)	−0.09091 (6)	2.67 (2)
P3	0.09795 (3)	0.1250 (1)	0.08991 (6)	3.17 (2)
O1	0.0608 (1)	−0.1173 (5)	−0.1190 (2)	7.7 (1)
O2	0.1388 (1)	−0.3351 (4)	0.0811 (2)	6.57 (9)
O3	0.1986 (1)	−0.2067 (4)	−0.1463 (2)	5.09 (7)
C′	0.250	0.000	0.1184 (3)	2.9 (1)
C1	0.0909 (1)	−0.0726 (6)	−0.0814 (3)	4.26 (9)
C2	0.1403 (1)	−0.2149 (5)	0.0445 (2)	3.66 (8)
C3	0.1793 (1)	−0.1289 (5)	−0.0984 (2)	3.21 (8)
C11	0.2313 (1)	0.2749 (5)	0.0153 (2)	3.19 (7)
C12	0.1982 (1)	0.3791 (4)	−0.0321 (2)	3.14 (7)
C13	0.1794 (1)	0.1964 (5)	0.1596 (2)	3.47 (8)
C14	0.1335 (1)	0.2636 (6)	0.1487 (3)	4.33 (9)
C21	0.1177 (1)	0.4145 (5)	−0.1140 (3)	3.73 (9)
C22	0.0812 (2)	0.3572 (6)	−0.1700 (3)	5.9 (1)
C23	0.1859 (1)	0.2283 (5)	−0.1889 (2)	3.55 (8)
C24	0.1969 (2)	0.3799 (6)	−0.2379 (3)	5.1 (1)
C31	0.0742 (2)	−0.0096 (6)	0.1671 (3)	5.0 (1)
C32	0.0397 (2)	−0.1267 (7)	0.1362 (4)	6.7 (1)
C33	0.0508 (2)	0.2577 (7)	0.0638 (3)	6.1 (1)
C34	0.0305 (2)	0.3595 (7)	0.1307 (4)	8.6 (2)

[a] Anisotropically refined atoms are given in the form of the isotropic equivalent displacement parameter defined as $(^4/_3)[a^2B(1,1) + b^2B(2,2) + c^2B(3,3) + ab(\cos\gamma)B(1,2) + ac(\cos\beta)B(1,3) + bc(\cos\alpha)B(2,3)]$.

Table IV. Positional Parameters for $W_2(CO)_6(eHTP)$

atom	x	y	z	B,Å²
W	0.14389 (1)	−0.01033 (3)	−0.01664 (2)	2.309 (4)
P1	0.20383 (6)	0.1055 (2)	0.0683 (1)	2.24 (3)
P2	0.15883 (6)	0.2556 (2)	−0.0893 (1)	2.58 (3)
P3	0.09823 (6)	0.1241 (2)	0.0913 (1)	3.06 (4)
O1	0.0602 (2)	−0.1127 (9)	−0.1172 (5)	7.3 (2)
O2	0.1402 (2)	−0.3350 (7)	0.0834 (4)	6.2 (2)
O3	0.1998 (2)	−0.2049 (7)	−0.1448 (3)	5.0 (1)
C′	0.250	0.000	0.1197 (6)	3.2 (2)
C1	0.0905 (3)	−0.070 (1)	−0.0796 (5)	4.0 (2)
C2	0.1413 (2)	−0.2144 (8)	0.0457 (5)	3.3 (1)
C3	0.1806 (3)	−0.1292 (8)	−0.0979 (4)	3.0 (1)
C11	0.2316 (2)	0.2775 (8)	0.0161 (4)	2.8 (1)
C12	0.1988 (3)	0.3805 (8)	−0.0310 (4)	3.2 (1)
C13	0.1788 (3)	0.1967 (9)	0.1613 (4)	3.6 (2)
C14	0.1331 (3)	0.264 (1)	0.1504 (5)	4.0 (2)
C21	0.1174 (3)	0.4151 (9)	−0.1113 (5)	3.6 (2)
C22	0.0814 (3)	0.356 (1)	−0.1691 (6)	5.9 (2)
C23	0.1856 (3)	0.2283 (9)	−0.1893 (5)	3.9 (2)
C24	0.1964 (4)	0.381 (1)	−0.2373 (5)	5.5 (2)
C31	0.0742 (3)	−0.0114 (9)	0.1679 (6)	4.8 (2)
C32	0.0401 (4)	−0.131 (1)	0.1350 (7)	6.9 (3)
C33	0.0513 (3)	0.257 (1)	0.0644 (6)	5.9 (2)
C34	0.0306 (4)	0.360 (1)	0.1325 (8)	8.4 (3)

[a] Anisotropically refined atoms are given in the form of the isotropic equivalent displacement parameter defined as $(^4/_3)[a^2B(1,1) + b^2B(2,2) + c^2B(3,3) + ab(\cos\gamma)B(1,2) + ac(\cos\beta)B(1,3) + bc(\cos\alpha)B(2,3)]$.

good electron-donating phosphine ligands is reflected in the positions of the carbonyl bands: 1910, 1820, and 1802 cm^{-1} for Cr; 1925, 1833, and 1808 cm^{-1} for Mo; and 1920, 1827, and 1805 cm^{-1} for W. These can be compared to that seen for the analogous mononuclear complexes $M(CO)_3$(triphos) (where M = Cr, Mo, W; triphos = $(Ph_2PCH_2CH_2)_2PPh$) which have carbonyl frequencies that are shifted to higher wavelengths by 10–20 cm^{-1}.[12,13]

The $^{31}P\{^1H\}$ NMR spectra are very similar to that found for $Co_2(CO)_4(eHTP)^{2+}$, unquestionably pointing to the

(12) (a) King, R. B.; Kapoor, P. N.; Kapoor, R. N. *Inorg. Chem.* **1971**, *9*, 1841. (b) King, R. B.; Zinich, J. A.; Cloyd, J. C. *Inorg. Chem.* **1975**, *14*, 1554.

(13) Chatt, J. C.; Watson, H. R. *J. Chem. Soc. A* **1970**, 3345.

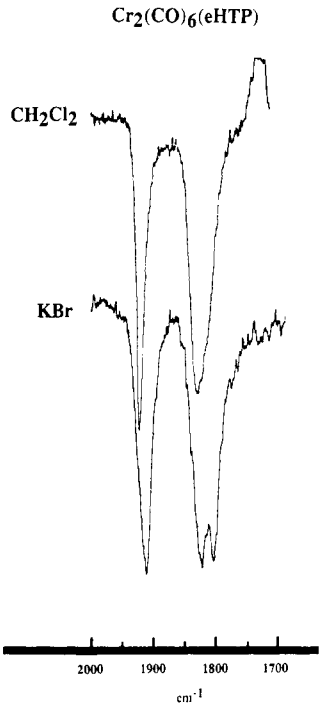

Figure 1. Infrared spectrum of the carbonyl region for $Cr_2(CO)_6$(eHTP).

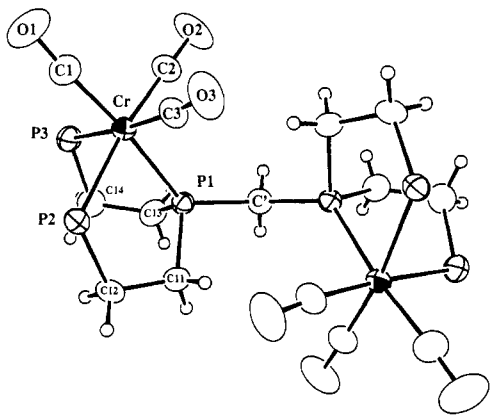

Figure 2. ORTEP plot of $Cr_2(CO)_6$(eHTP). ORTEP plots for the Mo and W structures are identical in appearance. Ethyl groups on the terminal phosphines have been omitted for clarity. The molecule sits on a crystallographic twofold rotation axis that passes through the central methylene bridge (C'). Thermal ellipsoids are shown at the 50% probability level.

more "traditional" open-mode eHTP configuration seen for that complex and not the less symmetrical structure seen for Cr_2Cl_6(eHTP) (**1d**). The internal phosphine resonance (107 ppm, 2 P) for **2** is downfield from that of the external phosphine signal (73 ppm, 4 P) which clearly indicates that the internal phosphines are involved in two five-membered chelate rings, while the external phosphines are involved in only a single five-membered chelate.[14] Simulation of the spectra using an $A_2XX'A'_2$ spin system leads to coupling constants considerably lower than those found in $Co_2(CO)_4$(eHTP)$^{2+}$: P_{inner}–P_{outer} = 16.8 Hz (47 Hz for Co) and P_{inner}–P_{outer} = 23.5 Hz (35 Hz for Co). All the spectroscopic data indicate a $M(CO)_3(P)_3$ facial coordination geometry with an open-mode eHTP conformation.

The X-ray structures on **2**, **3**, and **4** confirm the facial, open-mode assignments from the spectroscopic data.

(14) (a) Garrou, P. E. *Chem. Rev.* **1981**, *81*, 229. (b) Grim, S. O.; Barth, R. C.; Mitchell, J. D.; DelGaudio, J. *Inorg. Chem.* **1977**, *16*, 1776.

Table V. Bond Distances (Å) for $M_2(CO)_6$(eHTP) (M = Cr, Mo, W)

	Cr	Mo	W
M–M	6.2872 (8)	6.4687 (5)	6.4378 (5)
M–P1	2.3471 (8)	2.4862 (9)	2.480 (2)
M–P2	2.3849 (9)	2.5243 (9)	2.514 (2)
M–P3	2.3681 (9)	2.5125 (9)	2.505 (2)
M–C1	1.844 (4)	1.972 (4)	1.984 (8)
M–C2	1.819 (4)	1.959 (4)	1.954 (7)
M–C3	1.836 (3)	1.966 (4)	1.990 (7)
P1–C′	1.851 (2)	1.848 (2)	1.847 (5)
P1–C11	1.826 (3)	1.835 (4)	1.847 (6)
P1–C13	1.852 (3)	1.858 (4)	1.862 (7)
P2–C12	1.849 (3)	1.843 (3)	1.851 (7)
P2–C21	1.844 (3)	1.837 (4)	1.842 (7)
P2–C23	1.839 (3)	1.829 (4)	1.848 (8)
P3–C14	1.837 (4)	1.839 (4)	1.833 (9)
P3–C31	1.824 (4)	1.829 (4)	1.827 (8)
P3–C33	1.853 (4)	1.846 (5)	1.84 (1)
O1–C1	1.155 (4)	1.164 (5)	1.160 (9)
O2–C2	1.168 (4)	1.152 (4)	1.161 (9)
O3–C3	1.154 (4)	1.170 (4)	1.148 (8)
C11–C12	1.520 (4)	1.530 (5)	1.51 (1)
C13–C14	1.519 (5)	1.508 (5)	1.50 (1)
C21–C22	1.527 (6)	1.516 (6)	1.52 (1)
C23–C24	1.516 (6)	1.514 (6)	1.51 (1)
C31–C32	1.510 (7)	1.507 (7)	1.52 (1)
C33–C34	1.509 (8)	1.512 (9)	1.54 (1)
C′–P1	1.851 (2)	1.848 (2)	1.847 (5)

[a] Numbers in parentheses are estimated standard deviations in the least significant digits.

Table VI. Bond Angles (deg) for $M_2(CO)_6$(eHTP) (M = Cr, Mo, W)

	Cr	Mo	W
P1–M–P2	81.50 (3)	79.05 (3)	79.02 (6)
P1–M–P3	83.32 (3)	80.70 (3)	80.72 (6)
P1–M–C1	173.0 (1)	171.6 (1)	170.6 (3)
P1–M–C2	92.2 (1)	93.4 (1)	93.2 (2)
P1–M–C3	99.0 (1)	99.1 (1)	98.9 (2)
P2–M–P3	94.72 (3)	93.35 (3)	93.55 (6)
P2–M–C1	95.0 (1)	96.6 (1)	96.3 (2)
P2–M–C2	172.2 (1)	171.8 (1)	171.5 (2)
P2–M–C3	89.5 (1)	90.0 (1)	89.8 (2)
P3–M–C1	90.9 (1)	92.5 (1)	91.6 (3)
P3–M–C2	89.1 (1)	88.5 (1)	88.6 (2)
P–M–C3	175.5 (1)	176.6 (1)	176.4 (2)
C1–M–C2	91.8 (2)	91.3 (2)	91.9 (3)
C1–M–C3	87.0 (2)	88.0 (2)	89.1 (3)
C2–M–C3	86.9 (1)	88.1 (1)	87.9 (3)
C′–P1–C11	102.4 (1)	102.4 (1)	102.7 (3)
C′–P1–C13	96.3 (2)	96.3 (2)	96.7 (4)
C11–P1–C13	103.9 (2)	104.7 (2)	105.5 (3)
C12–P2–C21	98.9 (2)	99.4 (2)	99.3 (3)
C12–P2–C23	103.4 (2)	103.7 (2)	103.9 (4)
C21–P2–C23	101.7 (2)	102.1 (2)	102.1 (4)
C14–P3–C31	102.1 (2)	103.4 (2)	103.7 (4)
C14–P3–C33	103.7 (2)	102.6 (3)	102.1 (4)
C31–P3–C33	101.8 (2)	102.0 (3)	102.2 (4)
P1–C11–C12	110.1 (2)	111.1 (2)	111.0 (5)
P2–C12–C11	111.0 (2)	113.1 (2)	113.1 (4)
P1–C13–C14	113.5 (3)	114.7 (3)	115.1 (6)
P3–C14–C13	109.7 (2)	112.4 (3)	111.7 (5)
P2–C21–C22	113.8 (3)	113.8 (3)	112.9 (6)
P2–C23–C24	118.0 (3)	118.2 (3)	117.7 (6)
P3–C31–C32	115.4 (4)	114.7 (4)	114.3 (8)
P3–C33–C34	116.8 (4)	117.9 (6)	117.4 (8)
P1–C′–P1	126.6 (2)	125.3 (3)	125.5 (6)

These structures are isomorphous and possess a crystallographic twofold axis passing through the central methylene bridge. ORTEP plots for **2** are shown in Figures 2 and 3, while selected bond distances and angles for all three metals are listed in Tables V and VI. The geometry about the metal centers is, once again, octahedral with the expected distortions away from octahedral. The P–M–P

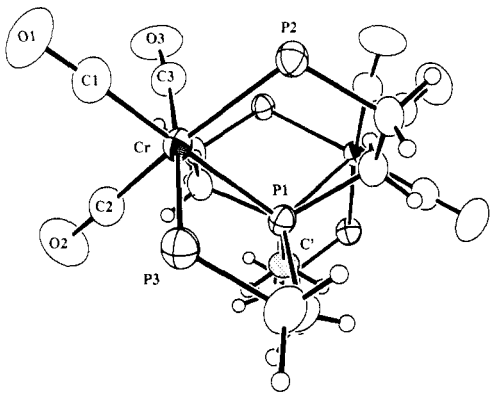

Figure 3. ORTEP plot of $Cr_2(CO)_6(eHTP)$ showing a view looking down the P1···P1′ axis to clearly show the rotational orientation of eHTP. The M-P1···P1′-M′ torsional (dihedral) angle for all three structures is 102°. The central methylene group, C′, has been dotted to highlight it as a reference point.

angles are contracted with the W and Mo systems having the smallest angles because the M–P bonds are approximately 0.14 Å longer than the Cr–P bonds. The metal coordination sphere trends are extremely similar to those seen for crystal structures on the mononuclear $M(CO)_3$(triphos) (M = Cr, Mo) complexes.[15] The structure on the tungsten complex, moreover, represents the first such structure on a $W(CO)_3(P_3)$-type system.

Although the eHTP ligand is in an open-mode configuration, it is not the same seen for the cobalt carbonyl complex $Co_2(CO)_4(eHTP)^{2+}$ which has the rather unusual inverted, W-shaped conformer **1b**.[2] The group VI complexes, on the other hand, have a eHTP open-mode conformation that is more closely related to that seen for the palladium and platinum complexes $M_2Cl_2(eHTP)^{2+}$ in which both metal centers are on the opposite side of the central methylene group hydrogen atoms. It is somewhat difficult to come up with a proper nomenclature for identifying the various rotamers for the eHTP ligand, but we have used the syn and anti notations in describing our nickel system and will, for lack of a better system, continue with this nomenclature.[5] Syn will, therefore, refer to when a metal atom is on the same side of the eHTP ligand as the central methylene group hydrogen atoms, while anti will indicate that the metal atom is on the opposite side. The $Co_2(CO)_4(eHTP)^{2+}$ structure **1b** is therefore designated syn–syn, while the $Ni_2Cl_2(eHTP)^{2+}$ structure **1c** is called syn–anti ("up–down").

The $M_2(CO)_6(eHTP)$ structures described here are of the anti–anti type, although still quite far away from the ultimate anti–anti closed-mode conformation **1a** as indicated by the long metal–metal distances: Cr–Cr = 6.2872 (8), Mo–Mo = 6.4687 (5), and W–W = 6.4378 (5) Å. The rotational orientation can be more clearly seen in Figure 3 which shows a perpendicular view from that in Figure 2 looking down the P1–P1′ axis. The M–P1···P1′–M′ torsional (dihedral) angle is ca. 102° for all three dimers. This can be compared to the partially closed-mode $M_2Cl_2(eHTP)^{2+}$ (M = Pd, Pt) dimers where there are considerably smaller M1–P1···P4–M2 torsional angles of 58° and 62° (0° represents a closed-mode conformation) and M–M separations of 4.4217 (8) and 4.6707 (9) Å for Pd and Pt, respectively.[6,7] Another important parameter to consider for eHTP complexes is the bond angle of the central P–CH_2–P linkage which varies from 93.8 (2)°, in the mononuclear $FeCl(CO)(\eta^4\text{-eHTP})^+$ system,[16] to the extremely large value of 129.8 (9)° in the $Pt_2Cl_2(eHTP)^{2+}$ complex. The P–CH_2–P angles for these dimers are 126.6 (2)°, 125.3 (3)°, and 125.5 (6)° for Cr, Mo, and W, respectively, and are indicative of the considerable steric interactions involved in these complexes. This can be contrasted to the value of 115.2 (4)° seen for $Cr_2Cl_6(eHTP)$ which represents a "normal" methylene bridge angle for a bis(phosphino)methane type unit.[9]

Conformational Studies. At first glance the differences between the syn–syn eHTP configuration observed for the cobalt system and the anti–anti seen here for the group VI complexes may appear puzzling. The explanation is obviously tied into intramolecular steric interactions with the primary factor that differentiates between syn–syn and anti–anti rotamers for five- or six-coordinate metal centers (in the absence of M–M bonding) being the angle between the external phosphine arms of the eHTP ligand. Qualitatively, angles less than about 115° will favor the anti–anti orientation of the metal centers seen for the $M_2(CO)_6(eHTP)$ dimers reported here, while angles greater than around 125° should favor the inverted syn–syn conformation seen for $Co_2(CO)_4(eHTP)^{2+}$. Our van der Waals energy calculations on the nickel eHTP complex, which has a P_{ex}–Ni–P_{ex} angles of 158° and 166°, demonstrate that the closed-mode configuration, i.e., the ultimate anti–anti rotamer, is completely inaccessible primarily because of severe steric interactions between the external phosphine alkyl substituents from one half of the dimer to the other.[5] Only by opening up the central methylene bridge angle to 126–129° and having only a *four-coordinate* metal center do the $M_2Cl_2(eHTP)^{2+}$ (M = Pd, Pt) complexes adopt a partially closed-mode, anti–anti configuration.

In order to probe the steric factors in the $M_2(CO)_6$(eHTP) compounds in more detail, we have made use of the SYBYL molecular mechanics/graphics program package to calculate van der Waals energies for various rotations about the central methylene bridge.[5,17] The results are summarized in Figure 4 which shows a portion of the 360° × 360° van der Waals energy map for a model complex of $Mo_2(CO)_6(eHTP)$ with the axes showing rotation angles about the two central P–CH_2–P bonds (the origin represents the closed-mode geometry **1a**) and the contours representing relative van der Waals energies in increments of 5 kcal/mol up to a maximum of 20 kcal/mol. The map is approximately symmetrical about the diagonal since the two halves of the $M_2(CO)_6(eHTP)$ molecule are related by the crystallographic twofold rotation axis that passes through the central methylene bridge. The slight asymmetries arise from the fact that the two five-membered chelate rings on one half of the complex do not have identical conformations.

Before we discuss the results, it is important to point out that the energies from the van der Waals energy calculation should be formally treated as approximate and qualitative in nature. Except for the two rotatable P–CH_2–P bonds, our model assumes a static molecule based on the geometric parameters obtained from the crystal structure. It has been demonstrated that van der Waals energies from the SEARCH routines in SYBYL for geometry optimizations in cyclic systems do not generally constitute a reliable criteria for choosing potential structures since they tend to overestimate atom–atom interactions in these nonoptimized systems.[18] The net result is that

(15) Favas, M. C.; Kepert, D. L.; Skelton, B. W.; White, A. H. *J. Chem. Soc., Dalton Trans.* **1980**, 447.

(16) Askham, F. R.; Saum, S. E.; Stanley, G. G. *Organometallics* **1987**, *6*, 1370.

(17) (a) Naruto, S.; Motoc, I.; Marshall, G. R.; Daniels, S. B.; Sofia, M. J.; Katzenellenbogen, J. A. *J. Am. Chem. Soc.* **1985**, *107*, 5262. (b) The SYBYL program set is available from TRIPOS Associates, Inc., 1699 S. Hanley Road, Suite 303, St. Louis, MO 63144.

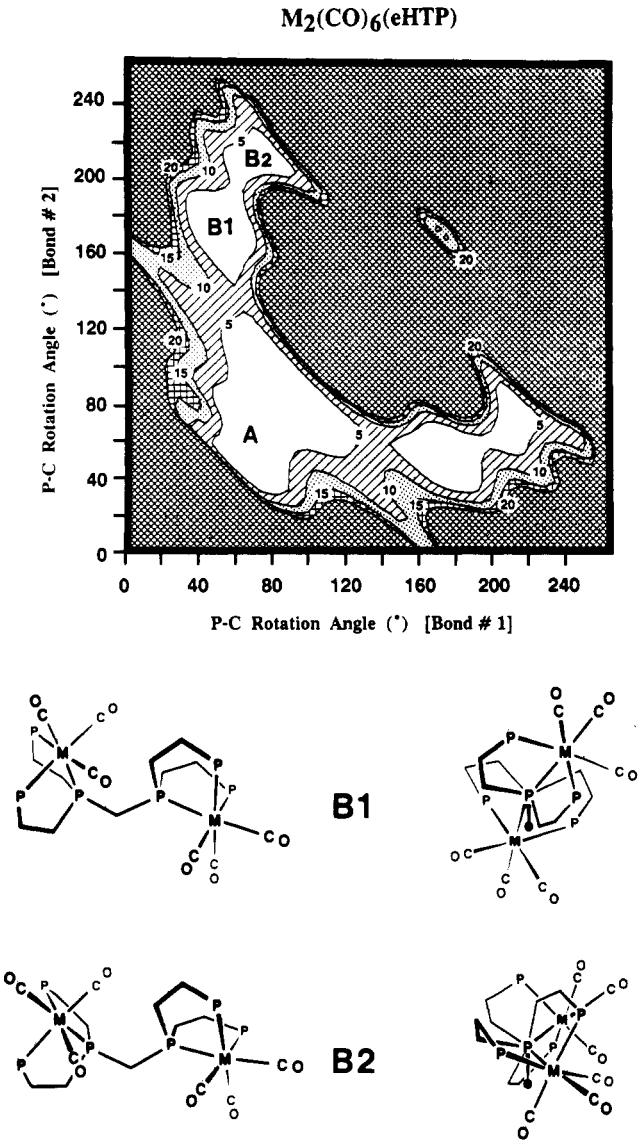

Figure 4. van der Waals energy map for a model complex of $Mo_2(CO)_6$(eHTP) with methyl groups on the terminal phosphine groups. Axes indicate rotational angles about the two P–CH_2–P bonds with contours depicting relative van der Waals energy values. The origin of the map (0°, 0°) represents the sterically inaccessible closed-mode geometry **1a**. Each contour represents 5.0 kcal/mol up to a maximum value of 20 kcal/mol. The map is symmetrical about the diagonal with the global minimum labeled A and the two other local minima labeled B1 and B2. The calculated position of A coincides almost exactly with the solid-state structure (see Figures 2 and 3). Conformations B1 and B2 are 0.7 and 2.1 kcal/mol higher in energy than A. Parallel and perpendicular views of conformations B1 and B2 are shown below the energy map, with the methyl groups on the terminal phosphines omitted for clarity and the central methylene group oriented down and emphasized in the perpendicular view by a heavy dot. Conformation B1 is proposed to be the species present in CH_2Cl_2 solution.

we can expect some of the higher van der Waals energies from the calculation to be overestimated. As we will see, however, this limitation on the accuracy of the van der Waals energies will not hinder our qualitative interpretations of the results.

Region A in Figure 4 is the location of the van der Waals energy global minimum, with the location of the label "A" marking the predicted most stable rotational configuration. This calculated minimum is nearly coincident with the rotational conformation observed in the crystal structure with only a 5° angular difference between the two. On the basis of the relatively large and flat contouring of region A, the calculation further indicates that there should be a fair bit of rotational flexibility about the central methylene linkage. Symmetrically opening up the P1–M···M′–P1′ torsional angle from 102° to 141°, for example, only increases the van der Waals energy by 2.6 kcal/mol. Rotation to the closed-mode geometry (0°, 0° in Figure 4) is, of course, forbidden because of the carbonyl ligands which completely block out this conformation.

The van der Waals energy calculation indicates that there is a second low-energy region which is labeled B in Figure 4. The position of the label B1 indicates the local minimum for this region and has a relative van der Waals energy of only 0.7 kcal/mol above that of the global minimum A. This conformation corresponds to a rotation about one of the P–CH_2–P bonds by approximately 110° to give a syn–anti configuration similar to **1b**. Parallel and perpendicular views of a stick representation of this conformation is shown in the lower portion of Figure 4. The M–P1···P1′–M′ torsion angle for this orientation is 156°, which is very similar to the observed eHTP ligand conformation and Ni–P1···P1′–Ni′ torsion angle of 146° seen for $[Ni_2Cl_2(eHTP)^{2+}]2BF_4^-$.[5] There is a second local minimum in region B which is located at the labeled position B2 in Figure 4 which has a relative van der Waals energy 2.1 kcal/mol and a M–P1···M′–P1′ torsion angle of 70°. A representation of this conformation is also shown at the bottom of Figure 4. This conformation approximately corresponds to the eHTP orientation seen for $[Ni_2Cl_2(eHTP)^{2+}]2Cl^-$ which has a M–P1···P1′–M′ torsion angle of 93°.

Importantly, the van der Waals calculation also gives us some idea about the pathway energetics for rotating from one conformation to another. The lowest energy barrier for rotation from conformation A to B1 is only 5.7 kcal/mol, indicating that there should be no steric problems in going from the observed solid-state configuration to that predicted for B1. Unlike the nickel system in which we could obtain different solid-state structures for the Cl^- and BF_4^- salts, which helped confirm the qualitative correctness of the SYBYL van der Waals energy calculations for that system, experimental evidence supporting the calculational results for this complex will be based on spectroscopic data.

The solution IR spectra (CH_2Cl_2) of **2**, **3**, and **4** do not show any splitting of the e-mode carbonyl band that is observed in the solid-state spectra (vide supra, Figure 1). We believe that this may be due to rotation about the central methylene group to give a rotational conformation similar to B1 in the van der Waals energy map (Figure 4). In the crystal structure the C3–O3 carbonyl group is just 4.78 Å away from the twofold related equivalent carbonyl group on the other half of the dimer, while the closest *intermolecular* CO–CO contact is 5.68 Å. This *intramolecular* CO–CO distance is close enough to allow the carbonyl groups to weakly interact and cause a splitting of the carbonyl e-mode in the IR spectrum. If the rotational conformation B1 becomes the global minimum in CH_2Cl_2 solution the results of the van der Waals energy calculation clearly indicate that the complex could easily rotate to adopt this orientation. Once in this configuration the carbonyl groups are now well separated with the closest CO–CO contact increasing to 6.7 Å, which is far enough away to effectively isolate each half of the dimer and give the expected simple two band carbonyl IR spectra observed in solution.

(18) Richards, A. (Tripos Associates), Tripos Users Meeting, St. Louis, MO, June, 1987.

It is particularly relevant at this point to compare these eHTP systems with King's related ethylene-bridged, phenyl-substituted hexaphosphine ligand $(Ph_2PCH_2CH_2)_2PCH_2CH_2P(CH_2CH_2PPh_2)_2$ (P_2(-Pf)$_4$).[19] This ligand is the progenitor of our eHTP ligand, but instead of being designed as a binucleating ligand such as eHTP, P_2(-Pf)$_4$ was intended to produce hexaligated phosphine *mononuclear* complexes analogous to EDTA. While no hexaligated M{P_2(-Pf)$_4$} complexes were prepared due to steric problems generated by the eight phenyl groups, a number of bimetallic complexes of P_2(-Pf)$_4$, including the $M_2(CO)_6${P_2(-Pf)$_4$} (M = Cr, Mo, W) family of compounds, were obtained.[19]

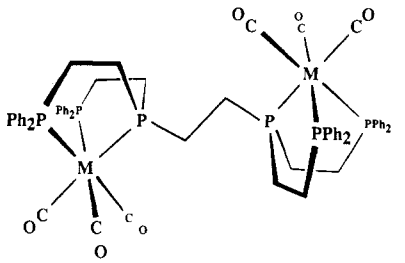

King's $M_2(CO)_6$(eHTP) (M = Cr, Mo, W) dimers have the two simple C_{3v} symmetry a_1 and e mode ν_{CO} bands at 1932 and 1830 cm^{-1} for Cr, 1932 and 1833 cm^{-1} for Mo, and 1930 and 1827 cm^{-1} for W.[19] There is no reported splitting of the e band, which according to the ideas discussed above indicates that there are no close intra- or intermolecular CO contacts that are lowering the symmetry enough to split this band. The absence of crystal structures on the $M_2(CO)_6${P_2(-Pf)$_4$} complexes, however, makes it quite difficult to experimentally confirm the P_2(-Pf)$_4$ ligand orientation in these systems.

We once again turned to the SYBYL van der Waals energy calculations to explore the conformational space for a $M_2(CO)_6${P_2(-Pf)$_4$} dimer system. Since there are no structures on these complexes, we used our $Mo_2(CO)_6$(eHTP) complex to build a model of $Mo_2(CO)_6${P_2(-Pf)$_4$}. As with the calculation on $Mo_2(CO)_6$(eHTP), we substituted the terminal phenyl groups with simple methyl groups and replaced the central methylene bridge with the ethylene bridge found in P_2(-Pf)$_4$. The three central ethylene bridge bonds (P–C, C–C′, and C′–P′) were selected for rotation, and the program did a 360° search in 30° increments about each bond evaluating the van der Waals energies at each orientation. The results fully confirmed our qualitative expectations: while there is a fair degree of rotational flexibility about the two central P–C bonds, the ethylene C–C orientation is essentially locked into an angle of 180°, which corresponds to a fully staggered ethane geometry. Thus, the two $(CO_3)Mo(P_3)$ halves of the molecule are well-separated, and there should be no close intramolecular CO–CO interactions or any splitting of the carbonyl e band in the IR induced by intramolecular effects.

(19) King, R. B.; Saran, M. S. *Inorg. Chem.* **1971**, *9*, 1861.

The other spectroscopic observation that may support the formulation of conformation B1 in solution is from the ^{1}H NMR. We have proposed that the position of the bridging methylene group hydrogen atoms in the $Co_2(CO)_4$(eHTP)$^{2+}$ complex is influenced by shielding effects from the proximal carbonyls.[2,20] In eHTP systems where there are no carbonyl shielding effects the methylene resonance is usually shifted downfield: $[Ni_2Cl_2$(eHTP)$^{2+}][Cl^-]$, 4.0 ppm (CH_2Cl_2), and FeCl(CO)(η^4-eHTP)$^+$, 4.3 ppm. In marked contrast the ^{1}H NMR signal for the methylene bridge in $Co_2(CO)_4$(eHTP)$^{2+}$ varies with temperature in acetone from 3.0 ppm at 52 °C to 3.6 ppm at −98 °C, while in CH_2Cl_2 this same peak is located at 2.38 ppm and is not particularly affected by temperature.[3] We believe that this shifting in position is caused by different rotational conformations of $Co_2(CO)_4$(eHTP)$^{2+}$ in solution which change the CO···H_2CP_2 contact distances and thus the magnitude of the carbonyl shielding effect.

The upfield position of the P–CH_2–P ^{1}H resonances in our $M_2(CO)_6$(eHTP) complexes (2.5–2.6 ppm) may point to the presence of some carbonyl shielding. Perhaps significantly, the CO···H_2CP_2 distance in conformation B1 is only 3.68 Å—close enough to cause a shielding effect.[20] This argument, however, remains somewhat tentative since it is not a simple matter to qualitatively predict the magnitude of the shielding effect, or even the cross over from shielding to deshielding. Additionally, one might expect that the methylene ^{1}H NMR resonances should be shifted upfield relative to the other cationic eHTP systems due to the neutral nature of our $M_2(CO)_6$(eHTP) compounds.

Except for a crystal structure on a closed-mode eHTP dimer, we believe that we have a reasonably good idea about the conformational preferences and dynamic properties of these binuclear systems. Our interest is now directed toward exploring the reaction chemistry of our eHTP complexes and the design of new polyphosphine ligands for imposing bimetallic complexes with unusual geometries. We are currently investigating the reaction chemistry of these $M_2(CO)_6$(eHTP) compounds, particularly with respect to their photochemical activity, and will report the results in an upcoming paper.[21]

Acknowledgment. We wish to thank the National Science Foundation (CHE-8613089) for supporting this research.

Registry No. **2**, 114221-40-8; **3**, 114221-41-9; **4**, 114221-42-0; $Cr(CO)_6$, 13007-92-6; $Mo(CO)_6$, 13939-06-5; $W(CO)_6$, 14040-11-0; $Cr(CO)_3$(cycloheptatriene), 12125-72-3.

Supplementary Material Available: A figure of the ^{1}H NMR spectra for $M_2(CO)_6$(eHTP) (M = Cr, Mo, W) and tables of anisotropic thermal parameters and hydrogen atom coordinates for the Cr and Mo structures (6 pages); a listing of observed and calculated structure factors (39 pages). Ordering information is given on any current masthead page.

(20) McGlinchey, M. J.; Burns, R. C.; Hofer, R.; Top, S.; Jaouen, G. *Organometallics* **1986**, *5*, 104.

(21) Saum, S. E.; Fronczek, F. R.; Stanley, G. G., manuscript in preparation.